CHAPTER 5

Probability-Based Seismic Assessment: Non-linear Dynamic Displacement Estimation in the Region of Global Instability

Jalayer, F. and Cornell, C. A. (2003 b). Earthquake Spectra, (in preparation).

5.1 Abstract

The demand and capacity factored design procedures discussed in the previous chapter, may break down in the region of global dynamic instability. This is the regime of large roof or other displacements where such displacements grow rapidly even for small increments in ground motion intensity. This chapter presents methods for determining the probability distribution for displacement demand that explicitly account for demand values reaching global instability. This probability distribution is usually conditioned on an appropriate seismic intensity measure, here, the spectral acceleration at the first mode period of the structure. The analysis methods discussed in the previous chapter can be modified for the estimation of the conditional probability distribution of displacement demand (given intensity) in the range of instability or "collapse" (e.g., "collapse" may be defined as global displacements beyond an arbitrary large value, or as lack of numerical convergence). This conditional probability distribution is used then in the implementation of probabilistic frameworks for seismic assessments. The mean annual frequency of exceeding a given maximum inter-story drift angle or "drift hazard" can be derived in various ways based on how the conditional probability distribution of drift demand given the spectral acceleration and the spectral acceleration hazard (the mean annual probability of exceeding a given spectral acceleration) are estimated. Factored demand and factored capacity were introduced in Chapter 3, as the main components of demand and capacity factored design (DCFD). A generalized definition of factored demand can be used to estimate the factored demand based on the estimated drift hazard curve. Factored capacity can also be estimated based on the estimated drift hazard and corresponding limit state probability. However, based on this definition, the factored capacity for the limit state of global collapse lies at infinity. Therefore, the modified DCFD design procedure taking into account the collapse information can be applied for seismic assessments only for limit states other than collapse or ("exogenous" limit states such as maximum local displacement limits). This study is presented through a comprehensive case study

of an existing reinforced concrete 7-story frame structure in Los Angeles, which is modeled with degrading strength in the nonlinear range.

5.2 Introduction

This chapter discusses the formulation and estimation of nonlinear dynamic displacement demand for probabilistic seismic assessments in the most severe ground motion regime, i.e., when the displacement demand is in the region of "global instability" in the structure. Global instability refers to a limiting case in structural response, namely, a mode of collapse when the global (dynamic) displacement response in the structure grows rapidly, i.e., the displacements increase an arbitrarily large amount for a (relatively) small increase in ground motion intensity. This limiting case in structural behavior, for a particular ground motion record can be marked by a point where the slope of the incremental dynamic analysis (IDA) curve decreases to a certain small percentage of its initial slope in the elastic region. Included too in global instability are the situations when the computer algorithm fails to converge. (See Chapter 4 or Vamvatsikos and Cornell (2001) for the description of an IDA curve).

In the previous chapter, we studied alternative methods for estimating the conditional probability distribution of displacement demand for a given intensity measure. We then calculated the demand hazard by integrating the estimated conditional distribution of displacement demand given the intensity measure and the hazard function for the intensity measure. An analytical closed-form expression was derived in Chapter 2 for the demand hazard assuming a parametric function (power-law) for the hazard and a lognormal distribution with constant dispersion for the conditional distribution of displacement demand. A demand and capacity factored design (DCFD) format was derived in Chapter 3 based on this analytical form. Factored demand, as introduced in Chapter 3, essentially forms one "half" of the formulation; the other "half" is the factored capacity. In chapter 4, we focused our attention on factored demand estimation. Building on a prior development in Chapter 3, factored demand was shown to be the demand value that corresponds to a hazard value equal to the allowable frequency of limit state (this demand value can be found from the demand hazard curve.). This equivalence property will be retained and will prove useful for the estimation of factored demand in this chapter.

Estimation of the conditional probability distribution for the displacement demand is pivotal in the demand estimation process. In Chapter 4, the distribution was typically modeled by a

lognormal distribution, which was used for the derivation of the closed form DCFD format; it was also estimated by a non-parametric empirical distribution which was used for the numerical integration calculations. However, for large values of ground motion intensity level, when the displacement demand approaches the region of global instability in the structure, a considerable portion of structural analysis results used for calculating the non-parametric percentiles produce arbitrarily large displacements. As a result, additional parameters may need to be introduced in order to reflect the portion of data in which the displacement response has become too large to be appropriately modeled by a common statistical model (e.g., log-normal). Shome and Cornell (1999) introduced a three-parameter distribution model in order to model the conditional probability distribution of displacement demand for a given intensity measure when cases of global instability (due to large deformations) are observed in the structural response. In this model, for a given intensity measure, the conditional probability distribution for non-collapse cases is modeled with a two-parameter lognormal distribution and a third parameter is introduced as the probability of collapse.

This chapter revisits some of the methods discussed in Chapter 4, this time considering explicitly global instability or "collapse" cases observed in the dynamic displacement response of the structure. The dynamic displacement response for the non-collapse portion of the sample of responses is modeled using the same statistical models discussed in Chapter 4. The additional variable accounting for the global instability is modeled both parametrically and non-parametrically. Parametric modeling is helpful for deriving a closed-form expression for demand hazard later in this chapter (similar to the DCFD presentation in Chapter 3), while non-parametric models are going to be useful for demand hazard estimation by numerical integration.

In the context of this study, the spectral acceleration of the fundamental period of the structure, S_a, is chosen to represent the ground motion intensity measure and the maximum inter-story drift, $\theta_{\max}$, represents the dynamic displacement-based demand. The methods discussed are equally applicable to other choices of the intensity measure and demand definitions.

5.3 Organization of this chapter

Chapter 4 was structured based on alternative analytical methods for the estimation of the displacement-based demand (here, the maximum inter-story drift angle), such as, single-stripe method or multiple-stripe method. This chapter, however is organized based on the quantities that

are being estimated, namely, the conditional drift demand, the drift hazard, and, the factored demand.

This chapter starts with a brief overview of spectral acceleration (the intensity measure) hazard estimation, as it will be the basis of future calculations. The next section discusses various ways in which the drift demand (displacement-based demand) can be estimated. The main purpose for demand estimation is to be able to estimate the conditional probability distribution of drift demand for a given spectral acceleration. The discussion of alternative methods for drift hazard estimation follows, as it is based on how the spectral acceleration hazard and the conditional probability distribution of drift demand for a given spectral acceleration are estimated. The demand and capacity factored design discussed in Chapter 4 is revisited, this time considering the global instability information in its formulation. Within this context, the alternative options for the estimation of the factored demand will be discussed.

Among the narrow-range and wide-range analysis methods discussed in Chapter 4, only single-stripe analysis, multiple-stripe analysis (MSA) and incremental dynamic analysis (IDA) are going to be used here as estimation tools.

Similar to the previous chapter, we have selected the transverse frame in a 7-story frame structure in Los Angeles, CA, as the case study frame structure. Information about modeling of this structure can be found in Chapter 4. Based on the static pushover results in Figure 4-3, we can anticipate that when maximum inter-story drift levels reach 1 to 2% or more, global instability may begin to be a threat. Further as we saw in the several figures there the curve of median maximum drift versus (dynamic intensity) first-mode spectral acceleration begins to curve and become much less stiff for drifts above about 1%, again implying that under some records (at least) the drifts are increasing rapidly as they do when under incipient dynamic instability. The nonlinear dynamic analyses are performed using the same selection of ground motion records described in the previous chapter. The selection consists of a set of 30 ground motion records selected from the Silva Catalog (Silva, 1998). These records were all California events recorded on stiff soil and were selected from a moment magnitude-(closest) source-to-site distance range of, $5.5 \le M \le 7.5$ and $15 \le R \le 120$.

5.4 Global dynamic instability capacity (collapse) estimation

In order to conduct studies in the region of global instability in the structure, we need first to estimate the drift demand values that represent the onset of global instability in the structure. For brevity, we will refer to these points as the "collapse cases".

We have used the results of the incremental dynamic analyses (see Chapter 4) in order to estimate the onset of global dynamic instability in the structure for each ground motion record. In this study, the onset of global instability is marked by the point where the local slope of the IDA curve decreases to a certain percentage (here 16.6% or less[1]) of the initial slope of the IDA curve in the elastic region (Figure 5-1-a and 5-1-b). Note that some of these maximum inter-story drift values are as low as 1 to 2 % but the majority lie in the 2 to 4% range.

1-a 1-b

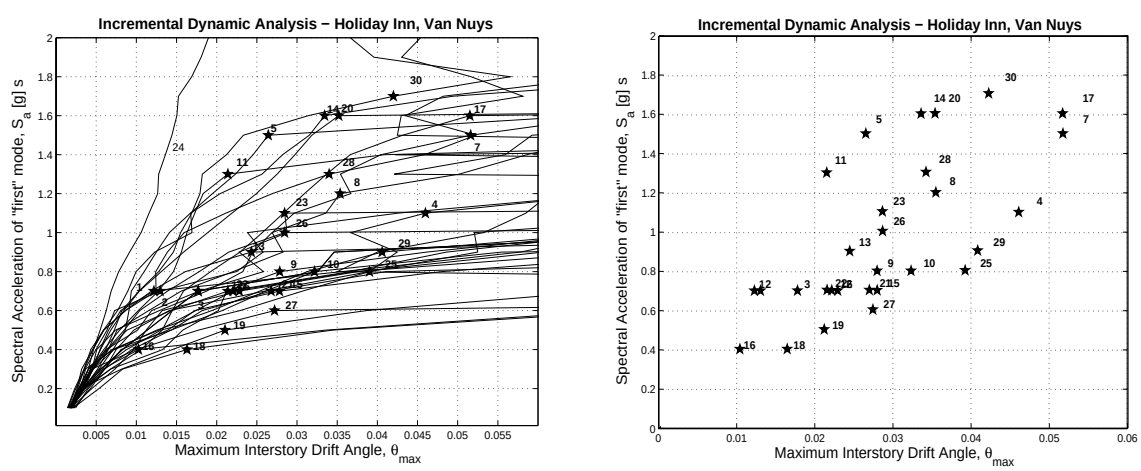

Figure 5-1 – Estimation of collapse points from IDA curves. a) IDA curves with the collapse points marked on them. b) Collapse Points plotted Separately.

Here we assume that for all spectral acceleration levels greater than the spectral acceleration capacity (the corresponding ordinate in the plot in Figure 5-1-b for each record), the structure has collapsed. Also, similar to FEMA 350 guidelines (SAC), we set an arbitrary upper bound (in SAC, it is a drift equal to 10%, here we set it equal to 5%) beyond which the model is surely

[1] Note that this percentage (16.6% or 1/6 of the elastic slope) is slightly less than the (20% or 1/5 of the elastic slope) used in the previous chapter. By decreasing the percentage, we were able to "catch" the corner point that precede a flat line in some of the IDA curves.

invalid. It should be noted that while this program (virtually always "converged", meaning that it produced a number) some programs do not. Such non-converging cases are also decidedly collapse cases.

5.5 Spectral acceleration hazard

The spectral acceleration hazard, i.e., the annual frequency of exceeding a given spectral acceleration, $\lambda_{S_a}(\cdot)$, can be represented both parametrically and non-parametrically. The hazard curve is normally described non-parametrically, which is the natural outcome of performing a site-specific probabilistic seismic hazard analysis (PSHA), as in the example in Chapter 4. A particular parametric formulation for the spectral acceleration hazard was introduced in the previous chapters (see also, Kennedy and Short, 1994, and, Luco and Cornell, 1998), in which the non-parametric spectral acceleration hazard curve was estimated (at least locally) by a power-law expression. Hence, at $S_a = x$:

$$\lambda_{S_a}(x) = k_0 \cdot x^{-k} \qquad (5\text{-}1)$$

5.6 Probability distribution of demand for a given spectral acceleration

As discussed above, we presented alternative methods for estimating the conditional probability distribution of drift demand for a given spectral acceleration in the previous chapter. This chapter focuses on demand estimations in the region of global instability in the structure. In order to model the distribution of demand in this region, we disaggregate the reported displacement response values into two groups: given non-collapse and given collapse groups. For example, given a spectral acceleration level of 0.5g, 3 of the 30 records have led to collapse. Thus, 27 records represent the "given non-collapse" group and 3 records the "given collapse" group for this ground motion level. All the alternative methods discussed in the previous chapter are still applicable for modeling the distribution of demand given non-collapse. The non-collapse estimations need to be supplemented with information about the conditional probability of collapse for a given spectral acceleration. This chapter presents both parametric and non-parametric methods for representing the conditional probability of collapse for a given spectral acceleration. Combining alternative methods for demand estimation introduced in Chapter 4 (here, for the non-collapse part), and the available options for estimating the conditional probability of collapse leads to a large variety of possibilities for estimating the distribution of demand in the region of global instability. We are not going to discuss all the possible options,

however. We shall only elaborate on those options that will be employed later for the estimation of drift hazard and factored demand.

For a given spectral acceleration, the conditional probability distribution function for drift demand in the region of the global instability in the structure can be estimated by parametric, semi-parametric and non-parametric methods, based on the methods used for modeling the distribution of non-collapse drift demand and the conditional probability of collapse.

Most of the methods discussed in this section incorporate a parametric statistical model known as the three-parameter distribution (Shome and Cornell, 1999) in their formulation. This model, estimates the distribution of the drift demand for a given spectral acceleration given that global instability is not happening (non-collapse cases), by a lognormal (two-parameter) distribution. It employs an additional (third) parameter to account for the probability of global instability (collapse) for a given spectral acceleration level. The conditional probability of collapse for a given spectral acceleration level, x, is denoted as:

$$P_{C|S_a}(x) = P[collapse \mid S_a = x] \qquad (5\text{-}2)$$

Equivalently, we can define the limit state of collapse in spectral acceleration capacity terms, i.e., collapse occurs when the spectral acceleration demand exceeds the (random variable) spectral acceleration capacity, $S_{a,C}$. Then, the conditional probability of collapse for a given spectral acceleration demand can also be written as:

$$P_{C|S_a}(x) = P[collapse \mid S_a = x] = P[S_{a,C} \le S_a \mid S_a = x] = F_{S_{a,C}}(x) \qquad (5\text{-}3)$$

where $F_{S_{a,C}}(x)$ is the cumulative distribution function (CDF) of the spectral acceleration capacity. This function is also known as a fragility function. A fragility function refers to a conditional probability of exceeding a limit state for a given intensity measure or demand parameter (for a discussion of fragility functions see Chapter 3 or Kennedy and Ravindra, 1984).

We dedicate the next few paragraphs to introducing the three-parameter distribution. This will be useful later when we discuss the alternative methods for estimating the conditional distribution of demand for a given spectral acceleration. Most of these methods employ the proposed three-parameter distribution for modeling the distribution of demand.

5.6.1 A Three-parameter distribution and its percentiles

Shome and Cornell (1999) expanded as follows the probability that drift demand, $\theta_{\max}$, exceeds a specified value, *y*, for a given spectral acceleration, x:

$$G_{\theta_{\max}|S_a}(y\,|\,x) = P[\theta_{\max} > y\,|\,S_a = x] = G_{\theta_{\max}|NC,S_a}(y\,|\,x)\cdot P_{NC|S_a}(x) + G_{\theta_{\max}|C,S_a}(y\,|\,x)\cdot(1-P_{NC|S_a}(x)) \quad (5\text{-}4)$$

where $G(\cdot)$ denotes the complementary cumulative distribution function (CCDF) and $P_{NC|S_a}(x)$ ($=1-P_{C|S_a}(x)$) is the probability of no collapse for a given spectral acceleration, x. Equation 5-4 is a special application of total probability theorem (see Appendix B or Benjamin and Cornell, 1970) expanding the probability of exceeding drift hazard based on whether the drift response has reached collapse (denoted by *C*) or not (denoted by *NC*). Given collapse, the conditional probability of exceeding any finite drift demand given collapse, $G_{\theta_{\max}|C,S_a}(\cdot)$, is assumed to be equal to 1:

$$G_{\theta_{\max}|C,S_a}(y\,|\,x) = P[\theta_{\max} > y\,|\,Collapse, S_a = x] = 1 \quad (5\text{-}5)$$

Using the above assumption, Equation 5-4 can be re-written as follows:

$$G_{\theta_{\max}|S_a}(y\,|\,x) = G_{\theta_{\max}|NC,S_a}(y\,|\,x)\cdot P_{NC|S_a}(x) + (1-P_{NC|S_a}(x)) \quad (5\text{-}6)$$

where $G_{\theta_{\max}|NC,S_a}(\cdot)$ is the CCDF of displacement demand, *y*, for a given spectral acceleration, *x*, given that no collapse cases has happened. Assuming that the drift demand distribution of non-collapse cases (for a given spectral acceleration) is lognormal, with median, $\eta_{\theta_{\max}|NC,S_a}$, and fractional standard deviation (i.e., standard deviation of the natural logarithm or dispersion), $\beta_{\theta_{\max}|NC,S_a}$. The CCDF, $G_{\theta_{\max}|NC,S_a}(\cdot)$, can be calculated as:

$$G_{\theta_{\max}|NC,S_a}(y\,|\,x) = P[\theta_{\max} > y\,|\,No\ Collapse, S_a = x] = \Phi^C_{\theta_{\max}|NC,S_a}\left(\frac{\ln(y)-\ln(\eta_{\theta_{\max}|NC,S_a}(x))}{\beta_{\theta_{\max}|NC,S_a}(x)}\right) \quad (5\text{-}7)$$

Where $\Phi^C(\cdot)$ is the standardized gaussian CCDF. Note that both the median and the dispersion are in general functions of S_a level, *x*. Substituting $G_{D|NC}(\cdot)$ with expression above (Equation 5-7) the CCDF for the drift demand given spectral acceleration, $G_{\theta_{\max}|S_a}(\cdot)$, is finally calculated as:

$$G_{\theta_{\max}|S_a}(y\,|\,x) = P[\theta_{\max} > y\,|\,S_a = x] =$$
$$\Phi^C_{\theta_{\max}|NC,S_a}\left(\frac{\ln(y) - \ln(\eta_{\theta_{\max}|NC,S_a}(x))}{\beta_{\theta_{\max}|NC,S_a}(x)}\right) \cdot P_{NC|S_a}(x) + (1 - P_{NC|S_a}(x)) \qquad (5\text{-}8)$$

Equation 5-8 demonstrates that the conditional probability distribution of drift demand for a given spectral acceleration is expressed by three parameters, namely, the conditional probability of no collapse, $P_{NC|S_a}(.)$, the median drift demand, $\eta_{\theta_{\max}|NC,S_a}(.)$, and the fractional standard deviation or dispersion of drift demand given no collapse, $\beta_{\theta_{\max}|NC,S_a}(.) = \sigma_{\ln\theta_{\max}|NC,S_a}(.)$, all functions of ground motion intensity level.

The CDF of the three-parameter distribution can be calculated after some simple algebraic manipulations and noting that $G(\cdot) = 1 - F(\cdot)$:

$$F_{\theta_{\max}|S_a}(y\,|\,x) = P[\theta_{\max} \le y\,|\,S_a = x] =$$
$$1 - G_{\theta_{\max}|S_a}(y\,|\,x) = \Phi_{\theta_{\max}|NC,S_a}\left(\frac{\ln(y) - \ln(\eta_{\theta_{\max}|NC,S_a}(x))}{\beta_{\theta_{\max}|NC,S_a}(x)}\right) \cdot P_{NC|S_a}(x) \qquad (5\text{-}9)$$

where $\Phi(\cdot)$ is the gaussian CDF. Equation 5-9 can be used in order to calculate the drift demand value, y_p, corresponding to percentile p of the three-parameter distribution, by setting the left side of the equation equal to p and solving it for y_p:

$$y_p(x) = F^{-1}_{\theta_{\max}|S_a}(p\,|\,x) = \eta_{\theta_{\max}|NC,S_a}(x) \cdot \exp(\beta_{\theta_{\max}|NC,S_a}(x) \cdot \Phi^{-1}_{\theta_{\max}|NC,S_a}(\frac{p}{P_{NC|S_a}(x)})) \qquad (5\text{-}10)$$

where $y_p(x)$ is the drift demand percentile for the spectral acceleration level x, i.e., the p% drift value, assuming that the probability distribution of the displacement response is estimated by the three-parameter distribution and $\Phi^{-1}(\cdot)$ is the inverse function of standardized normal distribution. Note that for $P_{NC|S_a}(x) = 1$, this leads to familiar formulas for 16th, 50th, and 84 percentiles of a lognormal distribution:

$$y_{0.16}(x) = \eta_{\theta_{\max}|NC,S_a}(x) \cdot \exp(-\beta_{\theta_{\max}|NC,S_a}(x))$$
$$y_{0.50}(x) = \eta_{\theta_{\max}|NC,S_a}(x)$$
$$y_{0.84}(x) = \eta_{\theta_{\max}|NC,S_a}(x) \cdot \exp(\beta_{\theta_{\max}|NC,S_a}(x)) \qquad (5\text{-}10\text{-a})$$

5.6.2 Methods incorporating the three-parameter distribution

In the section below, we discuss methods that incorporate the three-parameter distribution for modeling the conditional probability distribution of demand for a given spectral acceleration. These methods are differentiated based on how they estimate the (three) parameters of the three-parameter distribution.

5.6.2.1 Fully parametric using power-law functions

In this method, the parameters of the three-parameter distribution are all represented by analytical (parametric) functions that are assumed to apply at least locally in the region of interest. More practically, this means that they are accurate enough to provide adequate numerical estimates of the drift hazard, Equation 4-5-a, in some interval of drift levels of interest. The median drift demand for a given spectral acceleration given non-collapse, $\eta_{\theta_{\max}|NC,S_a}(.)$, is assumed to follow a power-law expression (e.g., Luco and Cornell, 1998, and, Cornell, Jalayer et al., 2002):

$$\eta_{\theta_{\max}|NC,S_a}(x) = \eta_{\theta_{\max}|NC,S_a=x} = a \cdot x^b \qquad (5\text{-}11)$$

The fractional standard deviation of drift for a given spectral acceleration given no-collapse is assumed in this model to be constant with respect to spectral acceleration:

$$\beta_{\theta_{\max}|NC,S_a}(x) = \beta_{NC} \qquad (5\text{-}12)$$

The parameters, a, b, and β_{NC} can be estimated for example, by simple regression applied to cloud or set of stripes of response results, as in Chapter 4, but now using only non-collapse data points. The conditional probability of non-collapse for a given spectral acceleration, $P_{NC|S_a}$, or the spectral acceleration fragility, $F_{S_{a,C}}(x)$, can be modeled by a power-law distribution (see Shome and Cornell (1999):

$$\begin{aligned} P_{NC|S_a}(x) &= 1 - F_{S_{a,C}}(x) = \left(\frac{x}{s_{a0}}\right)^{-\beta_C} & x > s_{a0} \\ P_{NC|S_a}(x) &= 1 - F_{S_{a,C}}(x) = 1 & x \le s_{a0} \end{aligned} \qquad (5\text{-}13)$$

The collapse points in Figure 5-1 can be used to estimate $P_{NC|S_a}$ empirically (e.g., by the ratio of the "collapse" points with a spectral acceleration greater than a given value, *x)*. The values of the two parameters, s_{a0} and β_c can be estimated, for example, by performing linear regression in the

logarithmic space on the empirical $P_{NC|S_a}$ values (Figure 5-2 and Table 5-1). If we substitute the above expressions in Equation 5-8, the CCDF for the drift demand given spectral acceleration, $G_{\theta_{\max}|S_a}(\cdot)$ will be written as:

$$G_{\theta_{\max}|S_a}(y\,|\,x) = P[\theta_{\max} \geq y\,|\,S_a = x] =$$
$$\Phi^C_{\theta_{\max}|NC,S_a}\left(\frac{\ln(y/a\cdot x^b)}{\beta_{NC}}\right)\cdot\left(\frac{x}{s_{a0}}\right)^{-\beta_C} + \left[1-\left(\frac{x}{s_{a0}}\right)^{-\beta_C}\right] \qquad x \geq s_{a0} \qquad (5\text{-}14)$$

and,

$$G_{\theta_{\max}|S_a}(y\,|\,x) = P[\theta_{\max} \geq y\,|\,S_a = x] = \Phi^C_{\theta_{\max}|NC,S_a}\left(\frac{\ln(y/a\cdot x^b)}{\beta_{NC}}\right) \qquad x \leq s_{a0} \qquad (5\text{-}15)$$

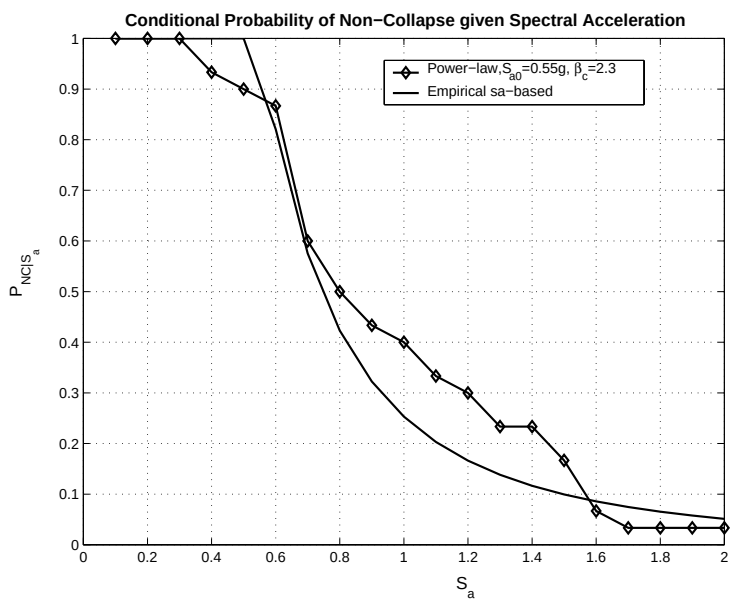

Figure 5-2 - Conditional probability of non-collapse for a given spectral acceleration represented both empirically and analytically.

s_{a0}	β_c
0.55g	2.3

Table 5-1. Parameter estimates for s_{a0} and β_c

For spectral acceleration values smaller than s_{a0}, the conditional probability distribution of drift demand for a given spectral acceleration is the same as the non-collapse conditional probability distribution. This is because, according to the model, the spectral acceleration value s_{a0} marks

the minimum spectral acceleration at which "collapse" cases can occur in the structure. In application, as in this example, there may be cases, e.g., $S_a = 0.55$, where there are observed collapses at S_a levels less than the estimated value of s_{a0}. Other methods of parameter estimation, e.g., maximum likelihood, could be used to avoid this inconsistency if it should prove unsatisfactory. The parametric model has the advantage that it can be estimated by results from as few as two S_a levels, implying savings in analysis runs. This property will be explored in a following section. Equation 5-14 will be used later in this chapter for the derivation of a closed-form result for the drift hazard considering now the global instability information.

5.6.2.2 Fully parametric using the IDA procedure

This method employs incremental dynamic analysis (IDA) to estimate the parameters of the three-parameter distribution. For a set of ground motion records, the results of incremental dynamic analysis of the structure are represented by the IDA curves. This new estimation method is based on the typical observation that the individual IDA curves in the non-collapse regime may each be relatively straight in a log-log representation but with quite widely varying slopes and intercepts (see Figure 5-3). The underlying probabilistic model is that each such curve is a straight line with *random* slope and intercept:

$$\ln \theta_{\max|NC,S_a}(x) = \ln A + B \cdot \ln x \qquad x \le S_{a,c} \qquad (5\text{-}16)$$

in which the intercept denoted by $\ln A$ (natural log of A) and slope b are assumed to be jointly normally distributed random variables with means, $\mu_{\ln A}$. and μ_B, and variances, $\sigma^2{}_{\ln A}$ .and $\sigma^2{}_B$, and correlation coefficient, ρ. The easily derived implications of this model are that $\theta_{\max|NC,S_a}(x)$ is log-normally distributed with median:

$$\eta_{\theta_{\max|NC,S_a}(x)}(x) = \eta_A \cdot x^{\mu_B} \qquad (5\text{-}17)$$

in which the η_A is the median of A (i.e., $\exp[\mu_{\ln A}]$), and fractional variance (i.e., variance of $\ln\theta$):

$$\beta^2{}_{\theta_{\max}|NC,S_a}(x) = \sigma^2_{\ln A} + 2 \cdot \ln x \cdot \rho \cdot \sigma_B \cdot \sigma_{\ln A} + (\ln x)^2 \cdot \sigma^2{}_B \qquad (5\text{-}18)$$

Note that unlike the model in previous section the fractional standard deviation is a function of spectral acceleration, not a constant.

The statistical parameters of $\ln A$ and b can be estimated as follows. For each record, i, fit (by regression) a line of the form, $\ln \theta_i(x) = \ln a_i + b_i \cdot \ln x$, to the nonlinear dynamic runs for all non-collapse cases, i.e., for $x \le S_{a,c_i}$, where S_{a,c_i} is the ith observed value of the S_a capacity random variable, i.e., the S_a level at which collapse is observed under the ith record. Then the sample values $\{\ln a_i, b_i\}$ for i=1,2,…,n, can be simply processed for the sample means, standard deviations and correlation coefficient, which can serve as estimates of the corresponding model parameters. Note that we are ignoring the variability of individual data points about each IDA line. Experience has shown that (in the non-collapse domain) this variability is quite small relative to the record-to-record variability of the fitted lines themselves. Figure 5-3 shows a few examples of such fitted lines. In fact, it is this small variability that implies that non-collapse portion of this method could be accurately implemented by as few as two non-linear analyses per record, which is a primary advantage it has.

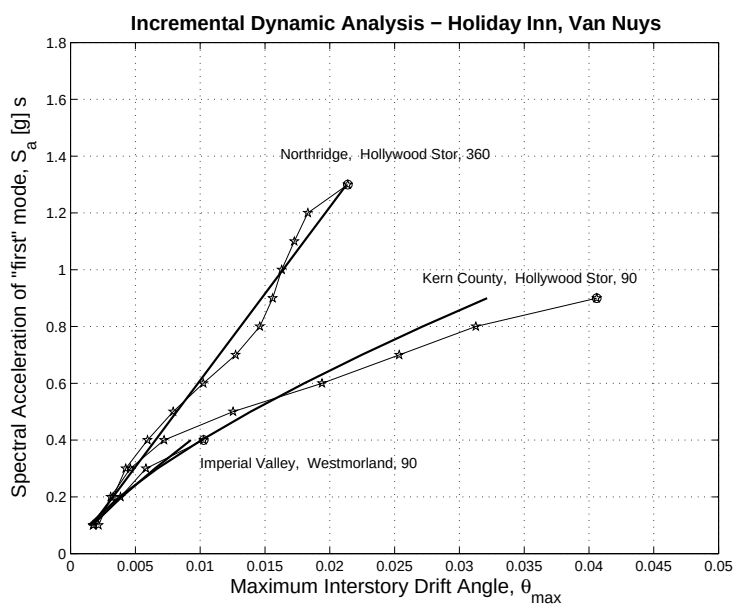

Figure 5-3 - Some IDA curves in the non-collapse regime approximated by straight lines in the log-log representation. Note that the points marked as circles in the end are the points at which the global instability capacity was reached (Figure 5-1)

The expression for the CCDF of drift demand for a given spectral acceleration $G_{\theta_{\max}|S_a}(\cdot)$ is similar to Equations 5-14 and 5-15, where the median and fractional standard deviation are calculated now from Equations 5-17 and 5-18. The conditional probability of no collapse

(Equation 5-13) is modeled and found as in the previous section. Figure 5-4 illustrates the 16th, 50th and 84th percentiles of the distribution of drift given spectral acceleration obtained by substituting the values for $\eta_{\theta_{\max}|NC,S_a}(.)$ and $\beta_{\theta_{\max}|NC,S_a}(.)$ from Equations 5-17 and 5-18 into Equation 5-10. The thin lines are the percentiles of the drift response (given spectral acceleration) obtained using the fully parametric IDA curves given no-collapse but ignoring the likelihood of collapse, i.e., by assessing s_{ao} in Equation 5-13 equal to infinity (i.e., as if this IDA-based method had been applied in Chapter 4 as it very well could have been). The thick lines are the percentiles using the fully parametric IDA curves and incorporating the probability of collapse information. The consideration of collapse cases has caused the percentiles to bend and diverge from their corresponding no-collapse values. This approach and the information gathered from the percentiles are going to be incorporated in the factored demand estimation later in this chapter. The parameter estimates used in this example are given in Table 5-2.

η_A	β_A	μ_B	σ_B	ρ
0.025	0.43	1.23	0.19	0.93

Table 5-2. Statistical parameters for *ln A* and *B*

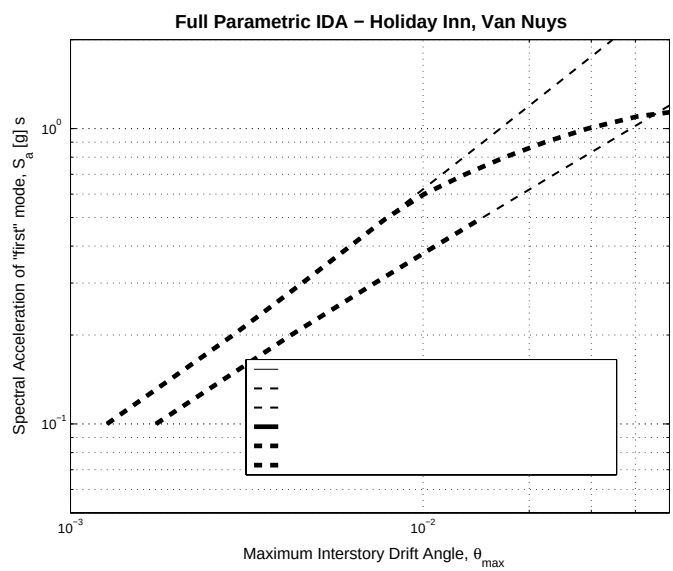

Figure 5-4 - Fully parametric 16th, 50th and 84th percentiles of the drift response given spectral acceleration obtained using parametric IDA curves.

5.6.2.3 Semi-parametric using multiple-stripe analysis

This method uses the results of the multiple-stripe analysis (revisited in Chapter 4) in order to estimate now the parameters of the three-parameter distribution and hence the probability distribution of demand in the region of global instability. For a given set of records, the results of the multiple-stripe analysis on the structure are represented by a series of "stripes" that are plotted for multiple spectral acceleration levels. For each spectral acceleration level, *x*, the non-collapse part of the stripe response is modeled by a lognormal (parametric) distribution. Also, the proportion of the observed collapse cases in the stripe response is used to estimate the (conditional) probability of collapse for the given spectral acceleration level, *x*. In contrast to the previous sections of this chapter these three parameter distribution parameters are not represented by parametric functions of *x*, however.

The results of the multiple-stripe analysis on the structures are plotted in Figure 5-5. These results are the same as those obtained in the previous chapter. The collapse cases, i.e., those for which the S_a value exceeds $S_{a,ci}$ of that record, are marked as stars inside the circles.

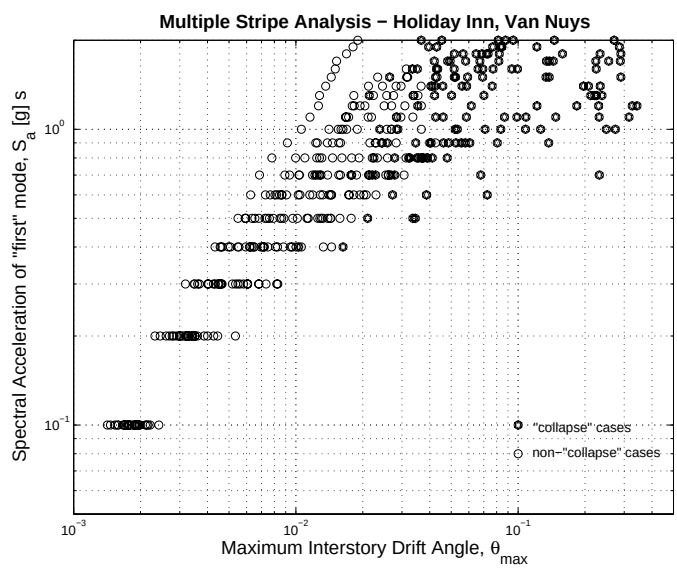

Figure 5-5 - Response results of multiple-stripe analysis with cases identified as collapse marked.

In order to fit a lognormal distribution to the non-collapse results for each spectral acceleration level, *x*, we need to estimate the median, $\eta_{\theta_{\max}|NC,S_a}(x)$, and the fractional standard deviation, $\beta_{\theta_{\max}|NC,S_a}(x)$. Here, we have estimated the non-collapse median, $\eta_{\theta_{\max}|NC,S_a}(x)$, by the (counted) 50th percentile of the non-collapse part of the stripe response. The non-collapse fractional

standard deviation, $\beta_{\theta_{\max}|NC,S_a}(x)$, is estimated in the logarithmic scale by half the distance between 16th and 84th percentiles of the non-collapse results. Note that the more conventional method of moments might have been used as well in this case. (The counted method has been used in the past largely to avoid the problems introduced by collapse-case data points, especially when these are associated with the non-convergence for which no observed value of $\theta_{\max}$ is available.) The conditional probability of non-collapse, $P_{NC|S_a}(x)$, for the stripe is estimated (empirically) by the ratio of the non-collapse cases to the total number response points on the stripe.

Having estimated the three parameters of the three-parameter distribution, as explained in the above paragraph, we can calculate the 16th, 50th and 84th percentiles of the marginal distribution in Equation 5-9 for each spectral acceleration level, *x*. Figure 5-6 illustrates these percentiles, as a function of the spectral acceleration, against the multiple-stripe analysis results in the background. The heavy lines stop when the probability of collapse becomes so large as to leave them undefined. The probability of collapse exceeds 50% above 0.7 g.

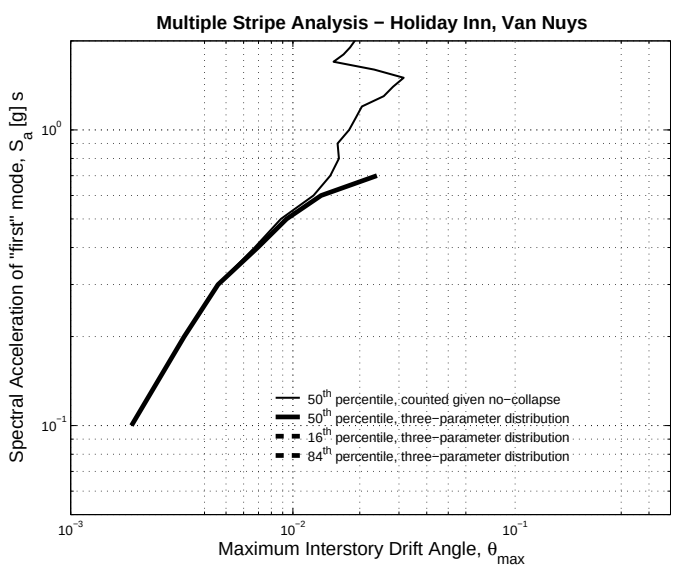

Figure 5-6 - The 16th, 50th and 84th percentiles of the semi-parametric three-parameter distribution calculated from the results of the multiple-stripe analysis.

5.6.2.4 Pseudo-parametric method

An alternative way to consider the collapse cases in the estimations is to fit a two-parameter lognormal distribution to the estimated percentiles. In this method, which we refer to as the pseudo-parametric approach, the 16th, 50th and 84th percentiles of the three-parameter distribution (calculated from Equation 5-10) are used to estimate the (two) parameters of the lognormal distribution, namely, the conditional median and fractional standard deviation of the drift demand given spectral acceleration. The conditional median, $\eta_{\theta_{\max}|S_a}$, is estimated by the 50th percentile and the conditional factional standard deviation, $\beta_{\theta_{\max}|S_a}$, is estimated by half the distance between counted 16th and counted 84th percentiles in the logarithmic scale. We have just presented several methods for deriving the parameter values of the response based on the three-parameter distribution. In this pseudo-parametric approach, the estimated percentiles using these alternative methods are approximated by a lognormal distribution. This model should be used with caution since it is trying to represent a sample including both extreme values (the collapse cases) and moderate values (the non-collapse cases) by only two parameters. Nonetheless we are going to use this method for factored demand estimation later in this chapter, if only because it provides the opportunity to use the simple representation of factored demand in Chapter 4. We shall compare its estimates with those obtained more rigorously.

5.6.2.5 Comparison of the fully-parametric IDA method to the semi-parametric method with MSA

The counted 16th, 50th and 84th percentiles of the drift response given spectral acceleration obtained semi-parametrically (using multiple-stripe analysis) and fully-parametrically (using IDA) are compared in Figure 5-7.

We can observe that parametric percentiles are somewhat different from the semi-parametric percentiles especially at lower S_a values. Reasons for this difference include the fact that the power-law curve in Figure 5-2 is not a very good approximation for the empirical $P_{NC|S_a}$, that IDA fits are dominated here by the higher density of points at the higher S_a levels, and that the IDA method simply does not have the flexibility that the MSA method has. However, the advantage of using the fully parametric method for estimating the probability distribution of drift given spectral acceleration is that the resulting percentiles are smooth functions of spectral acceleration.

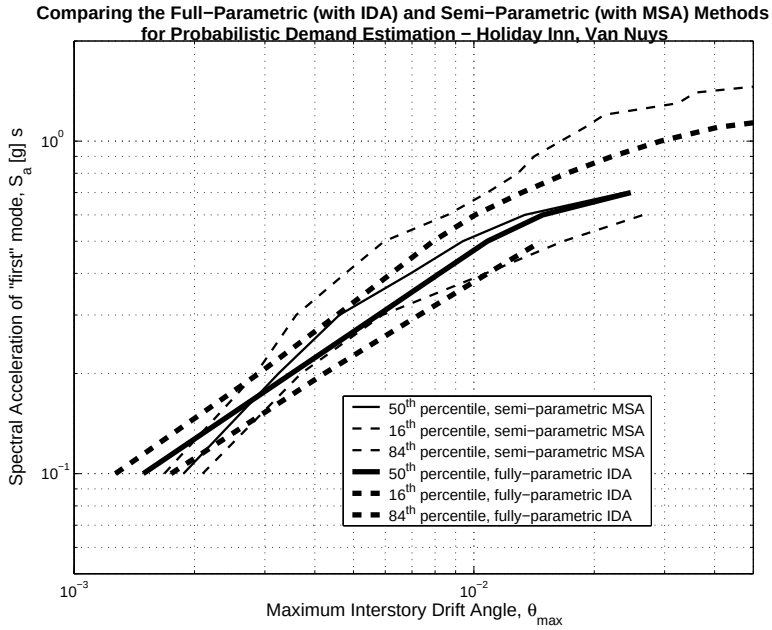

Figure 5-7 - The 16th, 50th and 84th percentiles of drift response given spectral acceleration estimated semi-parametrically using multiple-stripe analysis (MSA) and fully parametrically using the IDA procedure.

5.6.3 Non-parametric Methods

The methods that are discussed next do not explicitly use the three-parameter distribution for modeling the conditional probability distribution of demand for a given spectral acceleration. These methods simply estimate the counted percentiles of the drift demand given spectral acceleration using the results of multiple-stripe analysis.

The calculation of the counted percentiles involves sorting the reported drift results in ascending order. Therefore, the large drift values that correspond to collapse cases will move to the upper end of the sorted data and, hence, they will not enter the calculations as long as the desired percentile values exist (i.e., they have not yet reached the global dynamic instability limit).

5.6.3.1 Non-parametric considering the collapse cases

The non-parametric percentiles of the drift demand given the spectral acceleration can be calculated by treating the collapse cases similar to non-converging results. In other words the reported drift values that are beyond the drift capacity level (for each specific record) are

effectively set to infinity. When, for any spectral acceleration value, the number of such considered collapse cases is large enough, the percentile value becomes effectively infinite as well and we simply cut-off or stop reporting the percentiles at that point.

The non-parametric estimates can also be obtained for $G_{\theta_{\max}|NC,S_a}(y|x)$ and $p_{NC|S_a}(x)$. The CDF for the non-collapse part of the stripe response is estimated empirically by the fraction of the non-collapse results that are less than or equal to a given drift value. The probability of non-collapse is estimated empirically by the ratio of the non-collapse cases observed in the stripe response. This method will be applied later in this chapter for calculating the drift hazard by numerical integration.

5.6.3.2 Non-parametric not considering the collapse cases

In this method the percentiles of the drift response for a given spectral acceleration are calculated by counting as described above. The counted percentiles are calculated from the reported drift values ignoring the fact that some may be beyond the collapse drift levels, i. e., collapse or non-collapse is not considered or recognized. The counted percentiles obtained in the previous chapter were calculated this way.

5.6.3.3 Comparison of the non-parametric methods considering and not considering the collapse cases

Figure 5-8 illustrates the non-parametric (counted) percentiles of the drift response as a function of spectral acceleration for the two methods discussed above, namely, the methods considering and not considering the collapse cases. The two sets of percentiles are of course identical as long as the counted percentiles considering the collapse cases exist. It can be observed that the counted percentiles considering the collapse information are cut off when the percentage of non-collapse cases is less than the corresponding percentile. For example, the 50th percentile curve considering collapse is cut off at 0.7g. At this spectral acceleration level, some of the (relatively) smaller drift values were recognized as collapse cases, and this has slightly shifted the 50th percentile curve towards larger drift values. It is at higher S_a and drift levels, near collapse that differences emerge.

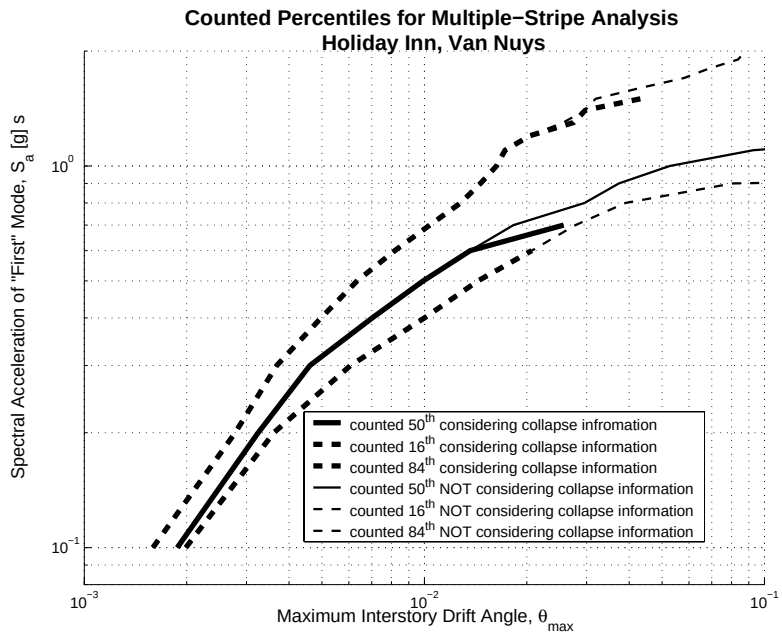

Figure 5-8 - Multiple-stripe analysis counted 16th, 50th and 84th percentiles of the response with and without consideration of the collapse information

5.6.3.4 Comparison of the non-parametric method not considering the collapse cases and semi-parametric method with multiple-stripe analysis

The counted 16th, 50th and 84th percentiles of the drift response as a function of the spectral acceleration (as in Chapter 4, not considering the collapse information) and the semi-parametric estimation of parameters of the three-parameter distribution using multiple-stripe analysis discussed in Section 5.6.2.3 are compared in Figure 5-9 below.

The median curves in the two cases are very close up to the cut-off point. The 16th and 84th percentiles are fairly close for the two cases especially when the drift values are small. It can be anticipated, however, that predictions associated with large drift values (beyond 2-3%)will be strongly affected. We shall see in Section 5.7.2 that, indeed the drift hazard results diverge in this (large drift) region.

5.6.3.5 Discussion

Several methods for estimating the conditional probability distribution of demand given spectral acceleration have been discussed. These methods have been classified based on the degree to which they use parametric estimations in their calculations. Obviously, not all the possible options have been presented. The attention has been focused on the methods that are going to be

used later in this chapter for the estimation for the drift hazard and factored demand. For this illustrative case at least, as shown in Figure 5-7, the percentiles for demand provided by the fully parametric method based on IDA procedure, are not very close to those of the semi-parametric method using MSA analysis. Nevertheless, the percentiles provided by the fully parametric method can be obtained with a relatively small amount of analysis effort and yet they provide smooth results.

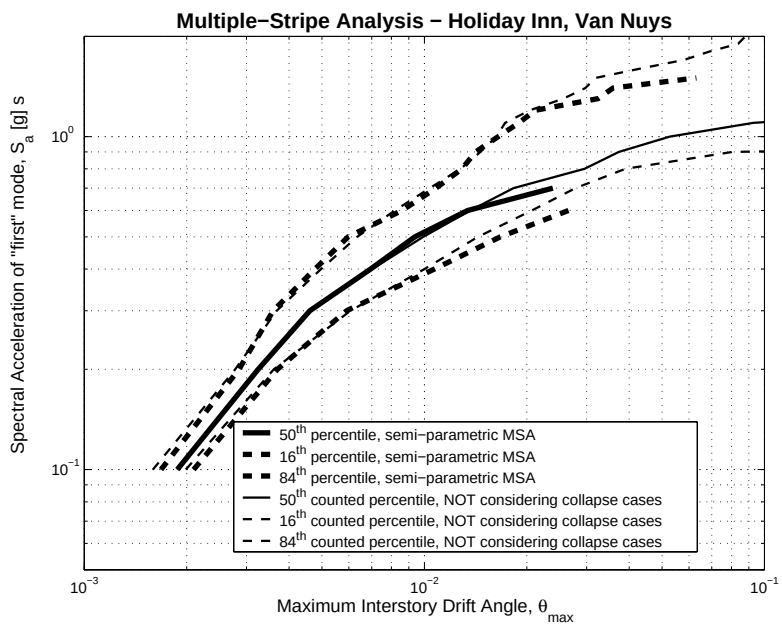

Figure 5-9 - The counted 16th, 50th and 84th percentiles not considering the collapse cases (as per Chapter 4) and the semi-parametric 16th, 50th and 84th percentiles using multiple-stripe analysis.

It is observed that the non-parametric counting method provides very good estimates at lower spectral acceleration/drift levels where there are few (if any) collapse cases. But deviations at large values may affect predictions, e.g., drift hazard at larger drift values in the collapse regime (to be seen in the next section). Nonetheless, the non-parametric counting methods still provide reasonable predictions in the near collapse regime, given their theoretical simplicity.

5.7 Drift Hazard – Annual Frequency of Exceeding Maximum Inter-Story Drift Demand

The drift hazard, or the mean annual frequency of exceeding maximum inter-story drift demand, $\lambda_{\theta_{\max}}(\cdot)$, when the drift demand is in the region of the global instability in the structure, can be estimated by parametric, semi-parametric and non-parametric methods. Based on how the spectral acceleration hazard and the probability distribution for demand given spectral acceleration are estimated, there are various possibilities for calculating the drift hazard. Only those that are more useful in the context of probabilistic seismic assessments in the region of global instability in the structure will be discussed here.

5.7.1 Estimating drift hazard by disaggregating into collapse and non-collapse parts

In the previous chapter, the drift hazard or the annual frequency of exceeding maximum inter-story drift demand was expanded with respect to the spectral acceleration as follows:

$$\lambda_{\theta_{\max}}(y) = \int_x G_{\theta_{\max}|S_a}(y \mid x) \cdot \left| \frac{d\lambda_{S_a}(x)}{dx} \right| \cdot dx \qquad (5\text{-}19)$$

Where $\lambda(\cdot)$ denotes the hazard function and $G_{\theta_{\max}|S_a}(\cdot)$ denotes the CCDF of maximum inter-story drift for a given spectral acceleration level.

While deriving the three-parameter distribution in the previous sections, we represented the CCDF of maximum inter-story drift for a given spectral acceleration level, $G_{\theta_{\max}|S_a}(\cdot)$, in the region of the global instability in the structure by Equation 5-6. Substituting that expression for $G_{\theta_{\max}|S_a}(\cdot)$ in the drift hazard equation in Equation 5-19, the drift hazard becomes:

$$\lambda_{\theta_{\max}}(y) = \int_x \{G_{\theta_{\max}|NC,S_a}(y \mid x) \cdot P_{NC|S_a}(x) + (1 - P_{NC|S_a}(x)\} \cdot \left| \frac{d\lambda_{S_a}(x)}{dx} \right| \cdot dx \qquad (5\text{-}20)$$

5.7.1.1 Drift hazard estimation in limiting cases

When the drift value, *y*, is very large, $G_{\theta_{\max}|S_a,NC}(y \mid x)$, the probability that the drift demand exceeds *y* given non-collapse, approaches zero for all spectral acceleration values, *x*. In this case, the drift hazard in Equation 5-20 becomes:

$$\lambda_{\theta_{\max}}(y) = \int_x (1 - P_{NC|S_a}(x)) \cdot \left| \frac{d\lambda_{S_a}(x)}{dx} \right| \cdot dx = \int_x P_{C|S_a}(x) \cdot \left| \frac{d\lambda_{S_a}(x)}{dx} \right| \cdot dx = \lambda_{LS} \qquad (5\text{-}21)$$

The expression for drift hazard in Equation 5-21, which is independent of the value *y*, is equal to the annual frequency of collapse limit state, λ_{LS}. Therefore, for large drift values, the drift hazard is asymptotically equal to the annual frequency of global instability limit state, λ_{LS} (or frequency of collapse).

When the drift value *y* is very small, $P_{NC|S_a}(y \mid x)$, or the probability of non-collapse for a given spectral acceleration, approaches to zero for all spectral acceleration values, *x*. In this case, the drift hazard in Equation 5-20 becomes:

$$\lambda_{\theta_{\max}}(y) = \int_x [G_{\theta_{\max}|NC,S_a}(y \mid x)] \cdot \left| \frac{d\lambda_{S_a}(x)}{dx} \right| \cdot dx = \lambda_{\theta_{\max}|NC}(y) \qquad (5\text{-}22)$$

Thus, for small drift values, the drift hazard is equal to the drift hazard assuming no collapse, which we denote by, $\lambda_{\theta_{\max}|NC}(.)$.

5.7.2 Non-parametric calculation of drift hazard by numerical integration

We can use the non-parametric method discussed in the previous section to estimate the CCDF of drift for a given spectral acceleration and given non-collapse, $G_{\theta_{\max}|S_a,NC}(.)$, and the conditional probability of non-collapse for a given spectral acceleration, $P_{NC|S_a}(.)$. The spectral acceleration hazard, $\lambda_{S_a}(.)$, can also be estimated non-parametrically as explained previously. Substituting the non-parametric estimates for $G_{\theta_{\max}|S_a,NC}(y \mid x)$, $P_{NC|S_a}(.)$ and $\lambda_{S_a}(.)$ into Equation 5-20, we can calculate the integral by numerical integration. This approach is parallel to the one used for the calculation of drift hazard by numerical integration in Chapter 4.

The drift hazard derived by numerical integration of Equation 5-20 is plotted versus spectral acceleration in Figure 5-10-a. In Figure 5-10-b, the drift hazard is plotted together with the drift hazard curve calculated non-parametrically by numerical integration without taking into account the "collapse" cases in the integration (as in Chapter 4). The two curves are identical for the low drift values where the probability of collapse given spectral acceleration is small. This is expected since the drift hazard given non-collapse is the upper limit for the drift hazard as discussed above.

The two curves start to diverge as the drift values become larger, when the drift hazard considering the collapse cases draws close to its lower limiting value, the annual frequency of collapse, λ_{LS}.

The probability of the global instability limit state in the structure can be estimated by the lower asymptotic limit of the drift hazard, as described in the previous section. Here, as the drift demand becomes large, the drift hazard gradually drops to a limiting value of $\lambda_{LS} = 0.007$. Thus, the general form of this drift hazard was anticipated and it deviates from that which would have been determined by methods presented in the previous chapter in the near collapse regime, here, for drifts of 1-2% and higher.

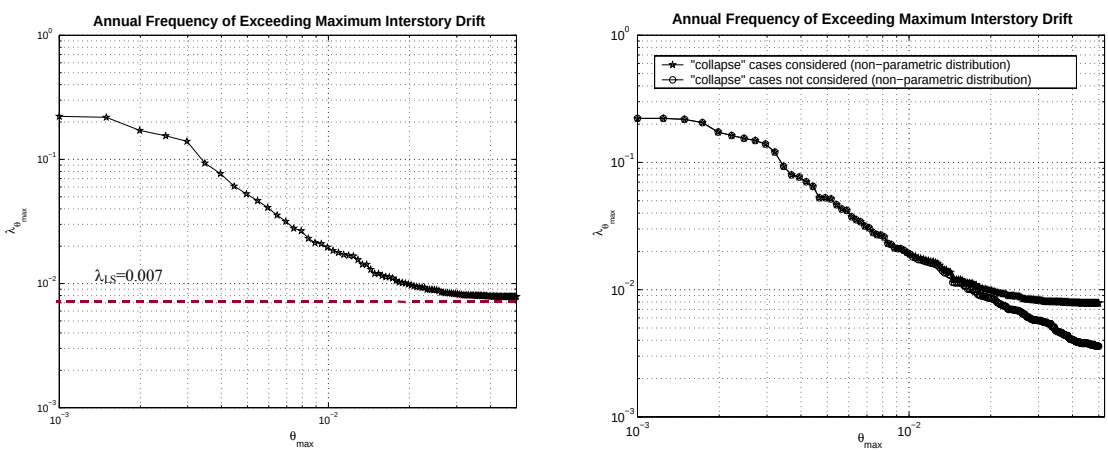

10-a 10-b

Figure 5-10 - Non-parametric estimation of drift hazard: a) "collapse" cases considered b) Plot 10-a together with drift hazard when the "collapse" cases are not considered.

5.7.3 Semi-parametric calculation of drift hazard by numerical integration using multiple-stripe analysis

The drift hazard can also be calculated by applying the semi-parametric method (using multiple-stripe analysis) for demand estimation. Recall for each stripe, the non-collapse median, $\eta_{\theta_{\max}|NC,S_a}$, and fractional standard deviation, $\beta_{\theta_{\max}|NC,S_a}$, are estimated in order to fit a lognormal distribution to the non-collapse part of the stripe response. This provides $G_{\theta_{\max}|S_a,NC}(.)$. The conditional probability of non-collapse for the stripe, $P_{NC|S_a}$, and the spectral acceleration hazard,

$\lambda_{S_a}(.)$, are both estimated empirically, as in the previous section. The drift hazard is calculated by numerical integration from Equation 5-20.

The semi-parametric drift hazard is plotted in Figure 5-11 together with the non-parametric drift hazard calculated in the previous section. The two curves illustrated in Figure 5-11 are so close that they may be used inter-changeably. This implies that the lognormal distribution is an adequate representation of the drifts given non-collapse.

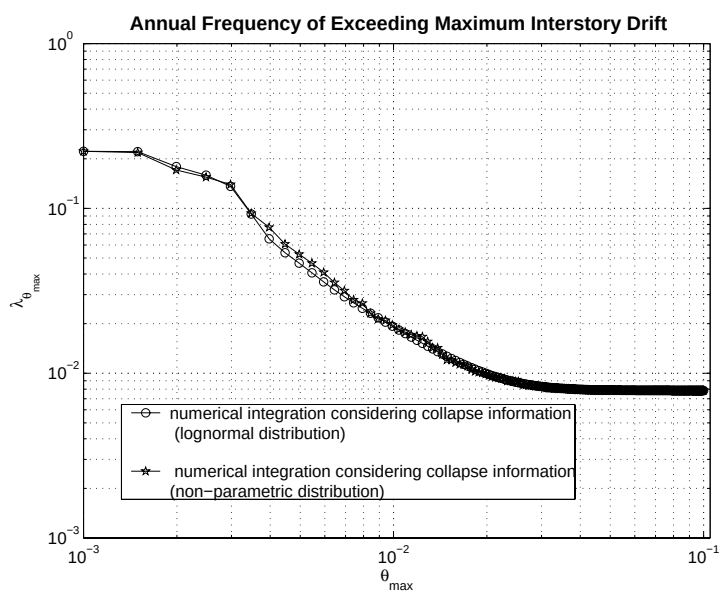

Figure 5 -11 - Drift hazard calculated by numerical integration using the non-parametric and semi-parametric (using the lognormal distribution for the non-collapse cases) methods.

5.7.4 Fully parametric (closed-form) evaluation of drift hazard

The fully parametric method for estimating the probability distribution of drift for a given spectral acceleration was introduced in a previous section (Equations 5-13 to 5-15). We use this method next to evaluate the drift hazard curve analytically. The conditional probability of non-collapse for a given spectral acceleration, $P_{NC|S_a}(.)$, can be modeled parametrically by the power-law form introduced in Equation 5-13. The spectral acceleration hazard, $\lambda_{S_a}(.)$, is also estimated parametrically from Equation 5-1. After substituting these estimates for $G_{\theta_{\max}|S_a,NC}(y\,|\,x)$, $P_{NC|S_a}(.)$ and $\lambda_{S_a}(.)$ in Equation 5-20 and carrying out the integral, a closed form expression for the drift hazard can be derived (for details of the derivation see Shome and Cornell, 1999):

$$\lambda_{\theta_{\max}}(y) = collapse\ \ term + \ non-collapse\ \ term1 + \ non-collapse\ \ term2 \qquad (5\text{-}23)$$

where:

$$collapse\ \ term = \frac{\beta_C}{k+\beta_C}\lambda_{S_a}(s_{a0})$$

$$non-collapse\ \ term1 = -\lambda_{S_a}(s_{a0})\cdot\Phi\left(\frac{b_{NC}\ \ln(s_{a0}/s_a^y)}{\beta_{NC}}\right) + \lambda_{S_a}(s_a^y)\cdot e^{\frac{1}{2}\frac{k^2}{b_{NC}{}^2}\beta_{NC}^2}\cdot\Phi\left(\frac{b_{NC}\ \ln(s_{a0}\cdot e^{\frac{1}{2}\frac{k}{b_{NC}}\beta_{NC}^2}/s_a^y)}{\beta_{NC}}\right)$$

$$non-collapse\ \ term2 = \frac{k}{k+\beta_C}\lambda_{S_a}(s_{a0})\cdot\Phi\left(\frac{b_{NC}\ \ln(s_{a0}/s_a^y)}{\beta_{NC}}\right) +$$

$$\frac{k}{k+\beta_C}\left(\frac{s_a^y}{s_{a0}}\right)^{-\beta_C}\cdot\lambda_{S_a}(s_a^y)\cdot e^{\frac{1}{2}\frac{(k+\beta_C)^2}{b_{NC}{}^2}\beta_{NC}^2}\cdot\Phi^C\left(\frac{b_{NC}\ \ln(s_{a0}\cdot e^{\frac{1}{2}\frac{k+\beta_C}{b_{NC}}\beta_{NC}^2}/s_a^y)}{\beta_{NC}}\right)$$

Where s_a^y is the spectral acceleration corresponding to the drift value, *y*, from the median curve (Equation 5-11), i.e.,

$$s_a^y = \eta^{-1}_{\theta_{\max}|NC,s_a^y}(y) \qquad \text{or more specifically: } s_a^y = \left(\frac{y}{a}\right)^{\frac{1}{b}}$$

The other parameters have been defined previously. Recall that *k is* a (log) slope parameter for the spectral acceleration hazard curve; *b* is a (log) slope parameter for the median drift demand curve (Equation 5-11) and β_C is a (log) slope parameter for $P_{NC|S_a}$ or spectral acceleration fragility function (Equation 5-13). s_{a0} is the fragility function parameter representing the minimum spectral acceleration value in which collapse cases are presumed to occur in the structure (Equation 5-13). β_{NC} is the constant fractional standard deviation of the non-collapse drift demand given spectral acceleration (Equation 5-12).

The consideration of collapse information makes the closed-form solution significantly more complicated than the DCFD formulation discussed in the previous chapter. It should also be noted that although Equation 5-23 gives a closed-form solution for the drift hazard when collapse information is being considered, it is not an analytical solution like the one in Chapter 4, due to

the (non-analytical) standardized Gaussian CDF, $\Phi(.)$, and its complement which appear in the formulation.

When the drift level y is low enough that s_a^y is small relative to s_{a0}, the drift hazard will be in this limit equal to the drift hazard given non-collapse:

$$\lambda_{\theta_{\max}}(y) = \lambda_{\theta_{\max}|NC}(y) = \lambda_{S_a}(s_a^y) \cdot e^{\frac{1}{2}\frac{k^2}{b^2}\beta_{NC}^2} \qquad (5\text{-}24)$$

This is the same form as in the previous chapter. On the other hand when y is such that s_a^y is large compared to s_{a0}, the drift hazard will in this limit be equal to the limit state of collapse frequency, λ_{LS}:

$$\lambda_{\theta_{\max}}(y) = \lambda_{LS} = \frac{\beta_C}{k+\beta_C}\lambda_{S_a}(s_{a0}) \qquad (5\text{-}25)$$

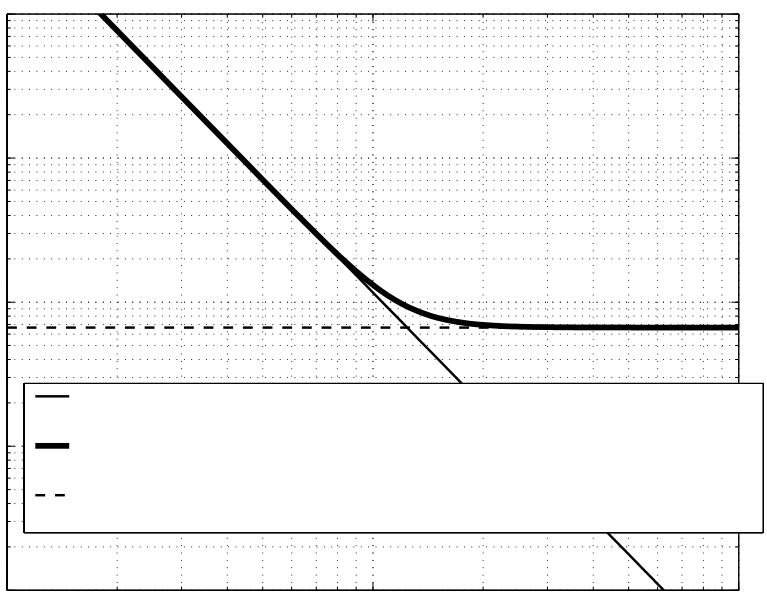

Figure 5-12 - Full-parametric drift hazard estimation using single-stripe analysis

Figure 5-12 illustrates a drift hazard calculated from Equation 5-23, using, s_{a0} and β_C values estimated in Figure 5-2 by fitting a power-law function to the empirical $P_{NC|S_a}$ data points, the a

and b and $\beta_{\theta_{\max}|NC}$ values close to the estimates given in Figure 4-10 (cloud analysis for the un-scaled records), and k and k_0 values by fitting a power-law to the hazard curve in the region of interest (near $S_a = 0.70g$). The figure also illustrates the limiting values for the drift hazard curve, namely, the drift hazard given non-collapse, $\lambda_{\theta_{\max}|NC}$, and limit state frequency, λ_{LS}.

5.7.5 Discussion

The drift hazard has been evaluated in this section by disaggregation of the drift response into collapse and non-collapse parts. Various methods for drift hazard estimation stem from this formulation, among which, several non-parametric, semi-parametric and fully parametric methods haven been discussed. The non-parametric method uses numerical integration to calculate the drift hazard. This method which relies on many runs at many closely spaced S_a stripes and hence many non-linear analysis runs, is the most reliable method for estimating the drift hazard among the methods discussed in this chapter. Hence, its resulting drift hazard curve is used in this chapter in order to measure the relative accuracy of the other methods, which in practice can be implemented with fewer dynamic analyses.

It is demonstrated that the non-parametric drift hazard curve considering the collapse cases is identical to the one that is calculated not considering the collapse cases until it starts to diverge and approach its minimum asymptotic value, the annual frequency of exceeding the collapse limit state (Figure 5-10). The semi-parametric method is very similar to the non-parametric method; it differs only in that it estimates the non-collapse CCFD of demand given spectral acceleration by a lognormal CCDF. As it is demonstrated in Figure 5-11, the resulting semi-parametric drift hazard curve is nearly identical to the non-parametric curve, proving that the lognormal assumption for the non-collapse CCDF of the response is a reasonable assumption in this case. A fully parametric closed-form solution for the drift hazard is presented at the end of this section. This formulation is parallel to the DCFD formulation presented in the previous chapter. Hence, it is going to be used in the next section for factored demand estimation.

5.8 Factored Demand

Factored demand, $F.D.$, was introduced in Chapter 4 as a part of the DCFD formulation for seismic assessment. When displacements are in the region of the global instability in the

structure, factored demand can be estimated by parametric, semi-parametric, pseudo-parametric and non-parametric methods.

Recall that we also observed in the previous chapter under the assumptions made there that the definition of factored demand for a given tolerable probability, p_o, is just equal to the drift value from the drift hazard curve corresponding to a hazard value equal to, p_o. The assumptions leading to the simple analytical DCFD formulation derived in Chapter 3 are not necessarily valid in the region of global instability. Hence, we propose here to use the alternative interpretation of factored demand, i.e., that which relates to drift hazard curve as a general definition of the factored demand.

5.8.1 Factored demand: Non-parametric using the non-parametric drift hazard

The non-parametric factored demand is calculated, using the general definition proposed above of factored demand, from the non-parametric drift hazard curve (Figure 5-10). According to this definition, the factored demand for an allowable limit state probability, p_o, is equal to the drift value corresponding to a drift hazard equal to p_o. This implies that the factored demand associated with a tolerable failure probability of p_o is equal to the drift demand with a mean annual frequency of exceedance of $\lambda_{\theta_{\max}} = p_0$ (recall annual probabilities and mean annual frequencies are numerically equivalent in this range). Further this definition means that the non-parametric factored demand curve plotted versus the acceptable probability values is the same as the non-parametric drift hazard curve in Figure 5-10. It should be noted that the factored demand in this case is read from the *x*-axis. Figure 5-14 is an example of such a curve re-labeled to emphasize this difference.

5.8.2 Fully-parametric using IDA procedure with simple DCFD formulation

The fully-parametric method for demand estimation was introduced in previous sections. In its pseudo-parametric form, this method provides a simple two-parameter lognormal approximation to the conditional distribution of demand given spectral acceleration even when there are collapse cases in the data set. Although this approach is not potentially favorable (for reasons discussed before), it is useful because it permits estimation of factored demand from the simple DCFD formulation (Equation 4-7):

$$Factored\ Demand = \eta_{\theta_{\max}|^{P_0}S_a} \cdot e^{\frac{1}{2}\cdot\frac{k}{b}\cdot\beta^2_{\theta_{\max}|S_a}} \qquad (5\text{-}26)$$

As described in the pseudo-parametric demand estimation method, we begin by deriving the full parametric 16th, 50th and 84th percentiles (Equation 5-10, the three-parameter distribution) of the drift response given spectral acceleration obtained using parametric IDA curves (Section 5.6.2.2), although other method such as MSA might also be used. Then, we use the full-parametric percentiles in order to estimate the median drift for a given spectral acceleration, $\eta_{\theta_{\max}|S_a}$, the conditional fractional standard deviation, $\beta_{\theta_{\max}|S_a}$, and the local b value. In order to estimate the local k value and the spectral acceleration hazard, $\lambda_{S_a}(.)$, we use the non-parametric spectral acceleration hazard curve.

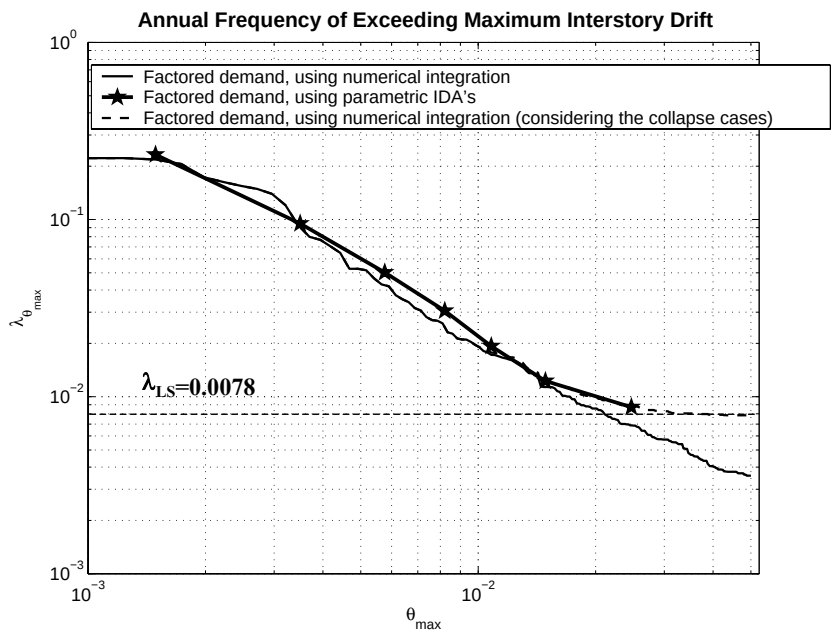

Figure 5-13 - Fully parametric factored demand estimation: Simple DCFD formulation using the parametric IDA curves and non-parametric spectral acceleration hazard

Here, we have estimated pseudo-parametric factored demand as described above and have plotted it in Figure 5-13. The non-parametric factored demand calculated by numerical integration is also plotted in the figure. We can observe that the pseudo-parametric factored demand stops at a drift value close to 0.024. This is due to the fact the parametric 50th percentile is only available up to a spectral acceleration level of 0.7g. However, as long as the pseudo-parametric estimation is available, there is close agreement between the two estimates for factored demand. This agreement looks promising, considering that the pseudo-parametric factored demand can be calculated with relatively little analysis effort compared to non-parametric factored demand

estimates. The relatively small analysis effort is attributed to the fact that the non-collapse parts of the IDA curves in the logarithmic scale are approximated with lines by performing regression. It is expected that the regression can result in reasonable estimates for the non-collapse IDA curves using fewer points than the several stripes of multiple-stripe analysis (as it is used for non-parametric factored demand estimation). Nonetheless, the method fails in the near-collapse regime (drifts larger than 1.5%) of primary interest here.

5.8.3 Factored demand: Semi-parametric using parametric IDA curves

We can employ the closed-form solution for the drift hazard considering the collapse cases in Equation 5-23, in order to calculate the factored demand. Figure 5-4 illustrates the full-parametric 16th, 50th and 84th IDA percentiles given non-collapse in thin lines. These non-collapse IDA percentiles are used to estimate the local median, $\eta_{\theta_{\max}|NC,S_a}$, fractional standard deviation of drift given spectral acceleration, β_{NC}, and b_{NC} value. The non-parametric spectral acceleration hazard curve is used to estimate the local *k* value and the spectral acceleration hazard, $\lambda_{S_a}(.)$.

We have incorporated the above estimations in Equation 5-23 and have plotted the resulting drift hazard in Figure 5-13. We have also plotted the non-parametric drift hazard curve for comparison.

The semi-parametric drift hazard curve illustrated above shows good agreement with the non-parametric drift hazard curve, especially for the drift values that are close to the range of global dynamic instability. However, the semi-parametric factored demand curve has a lower right asymptotic limit compared to the non-parametric factored demand. Similar to pseudo-parametric factored demand estimation in the previous section, the semi-parametric method uses linear regression to approximate the non-collapse portion of the IDA curves with lines in logarithmic scale. However, the semi-parametric method provides slightly better estimates for the factored demand compared to the pseudo-parametric method, since it is applying the (more elaborate) closed-form solution for drift hazard considering the collapse cases (Equation 5-23) instead of the simple DCFD formulation (Equation 5-24).

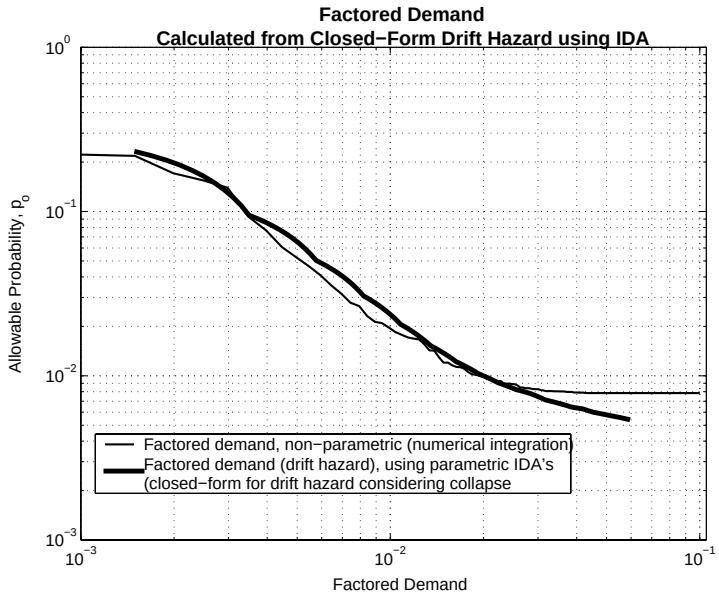

Figure 5-14 - Semi-parametric factored demand estimation: Using the closed-form for drift hazard in Equation 5-23 considering the collapse cases, with the parametric non-collapse (linear) IDA curves and non-parametric spectral acceleration hazard

5.8.4 Factored demand: Semi-parametric using single and double-stripe analysis

We have used the efficient single-stripe analysis in the previous chapter in order to estimate the factored demand for single limit state reliability assessments. This was possible since the drift hazard equation derived in the Chapter 2 (Equation 2-25) was invertible with respect to the drift values, and that resulted in an explicit formulation for the factored demand as a function of the allowable probability (Equation 5-26). Nevertheless, the single stripe analysis could not provide an estimate for the slope parameter, *b*. It was observed that the single-stripe analysis could provide accurate estimates of the factored demand provided that a reasonable value for the *b*-value was assumed. In this chapter, the estimation of factored demand is further complicated by the consideration of the collapse cases. The closed-form expression derived for the fully parametric drift hazard evaluation, Equation 5-23, is not invertible with respect to the drift value, *y*. Also, the number of parameters in the formulation increases. For example if we try to estimate the factored demand using a single-stripe analysis, we would have to assume value for the *b* value as well as two additional parameters that define the fragility function for the collapse capacity. Nevertheless, provided with the required parametric estimates, one could calculate the drift hazard curve from Equation 5-23 and then use the drift hazard curve to calculate factored demand as the drift value corresponding to a hazard value equal to p_o, i.e., factored demand for allowable probability, p_o. A double-stripe analysis (as per Chapter 3) may prove to be an adequate

estimation procedure, as with well chosen S_a values it can provide at least local estimates of all the six parameters necessary to calculate the drift hazard from Equation 5-23. In order for the estimates to be local, they need to be in the vicinity of p_o. Therefore, this approach may involve an additional iteration, and hence an additional single-stripe analysis. This method is called semi-parametric since it incorporates the non-parametric spectral acceleration hazard curve in the parametric formulation for the drift hazard curve. We outline as a step-by-step procedure for finding the factored demand using a double-stripe analysis.

- Determine the tolerable probability level, p_o.
- Estimate the *k* value. The *k* value can be estimated by the local (log) slope of the hazard curve in the vicinity of the allowable probability value, p_o.
- Calculate the spectral acceleration corresponding to p_o from the spectral acceleration hazard curve. Take the spectral acceleration of the first stripe equal to, ${}^{P_o}s_a$.
- Perform a single-stripe analysis at ${}^{P_o}s_a$.
- Check to see if there are collapse cases in the response. Two cases can happen:
  - *There is no collapse cases observed in the response.* calculate the drift hazard from the parametric expression for drift hazard given non-collapse (Equation 5-24). This requires assumption of a value for the slope parameter, *b*. Since there is no collapse case in the response, one may assume that the *b* value is equal to one, as per the equal displacement rule. In order to estimate the drift hazard in the vicinity of collapse one needs to repeat this first single-stripe analysis with a larger spectral acceleration value. This value should be large enough so that collapse cases are observed in its response.
  - *There are collapse cases observed in the response.* Find the conditional median and the fractional standard deviation of the stripe response given non-collapse, $\hat{\eta}_{\theta_{\max}|NC,S_a}({}^{P_o}s_a)$ and $\hat{\beta}_{\theta_{\max}|NC,S_a}({}^{P_o}s_a)$, respectively. Proceed to the next steps.
- Estimate $P_{NC|S_a}({}^{P_o}s_a)$, the probability of non-collapse at a spectral acceleration equal to ${}^{P_o}s_a$, as the fraction of the non-collapse cases in the stripe, $\hat{P}_{NC|S_a}({}^{P_o}s_a)$.
- Choose the spectral acceleration of the second stripe, s_a^2. Since we are interested in making estimations close to the collapse regime, the placement of the second stripe depends on the number of collapse cases observed in the response of the original stripe. If there are relatively few collapse cases, the spectral acceleration of the second stripe can be larger than that of the first stripe. If there are many collapse cases among the

responses, it is preferable to take the spectral acceleration of the stripe smaller than the first stripe. In both cases, it is useful to make sure that the two stripes are "sufficiently" spaced from each other in order to prevent the parameter estimates from being affected by possible local peculiarities. However, the spectral acceleration of the second stripe should be large enough so that there is at least one collapse case observed in the response. This is because the additional information provided by the second stripe is also going to be used for estimating the parameter estimates for the conditional probability of collapse for a given spectral acceleration, namely, s_{a0} and β_C. It should be noted that this procedure is implementing the double-stripe method outlined in the previous chapter.

- Perform the second single-stripe analysis at, s_a^2.
- Find $\hat{\eta}_{\theta_{\max}|NC,S_a}(s_a^2)$ and $\hat{\beta}_{\theta_{\max}|NC,S_a}(s_a^2)$.
- Estimate $P_{NC|S_a}(s_a^2)$ as the fraction of the non-collapse cases in the second stripe, $\hat{P}_{NC|S_a}(s_a^2)$
- Estimate the a_{NC} and b_{NC} (the later value as the slope of the line connecting the conditional median of the two stripes given non-collapse versus spectral acceleration, in the logarithmic space):

$$\hat{b}_{NC} = \left| \frac{\log\left(\dfrac{\hat{\eta}_{\theta_{\max}|NC,S_a}({}^{P_o}s_a)}{\hat{\eta}_{\theta_{\max}|NC,S_a}(s_a^2)}\right)}{\log\left(\dfrac{{}^{P_o}s_a}{s_a^2}\right)} \right| \quad \text{and} \quad \hat{a}_{NC} = \frac{\hat{\eta}_{\theta_{\max}|NC,S_a}({}^{P_o}s_a)}{\left({}^{P_o}s_a\right)^{\hat{b}_{NC}}}$$

- If the parameters s_{a0} and β_C were known, the conditional probability of non-collapse for the two stripes could be calculated from the following equations:

$$P_{NC|S_a}({}^{P_o}s_a) = \left(\frac{{}^{P_o}s_a}{s_{a0}}\right)^{-\beta_C} \qquad \text{for } {}^{P_o}s_a \geq s_{a0}$$

$$P_{NC|S_a}(s_a^2) = \left(\frac{s_a^2}{s_{a0}}\right)^{-\beta_C} \qquad \text{for } s_a^2 \geq s_{a0}$$

Since both stripes have collapse cases in them (as it is ensured in the preceding steps), their corresponding conditional probabilities of non-collapse are going to be described by the above equations that are specific to spectral acceleration levels higher than s_{a0}. Estimates of

the left hand sides of the two equations are available from prior steps. Therefore, s_{a0} and β_C can be calculated by solving the above equations, yielding:

$$\hat{\beta}_C = \left| \frac{\log\left(\frac{\hat{P}_{NC|S_a}({}^{P_o}s_a)}{\hat{P}_{NC|S_a}(s_a^2)}\right)}{\log\left(\frac{{}^{P_o}s_a}{s_a^2}\right)} \right| \quad \text{and} \quad \hat{s}_{ao} = \exp\left(\frac{\log(\hat{P}_{NC|S_a}({}^{P_o}s_a)) + \hat{\beta}_C \cdot \log({}^{P_o}s_a)}{\hat{\beta}_C}\right)$$

- Calculate the drift hazard from Equation 5-23 for a set of drift values close to $\hat{\eta}_{\theta_{\max}|NC,S_a}({}^{P_o}s_a)$ and $\hat{\eta}_{\theta_{\max}|NC,S_a}(s_a^2)$ and plot the resulting drift hazard curve.
- Find the drift value that corresponds to a drift hazard equal to p_o. This is the factored demand for an allowable probability equal to p_o. This is only possible if the range of the drift hazard values is wide enough to contain p_o.
- In case the factored demand calculated is too "far" from the drift values, $\hat{\eta}_{\theta_{\max}|NC,S_a}({}^{P_o}s_a)$ and $\hat{\eta}_{\theta_{\max}|NC,S_a}(s_a^2)$, then another iteration or at least another single-stripe analysis may be necessary.

As an example, we have used the procedure outlined above to calculate the factored demand for an allowable probability of, $p_o = 0.0088$, which corresponds to a spectral acceleration equal to, ${}^{p_o=0.0088}s_a = 0.70g$. First, we have obtained the local parameter estimates in the expression for drift hazard (Equation 5-23), following the steps above. The second stripe was chosen at $s_a^2 = 0.60g$. The factions of collapses in these two stripes were 0.4 and 0.13 (Figure 5-2), respectively. Estimated parameter values are $\hat{\eta}_{\theta_{\max}|NC,S_a}({}^{P_o}s_a)$ and $\hat{\eta}_{\theta_{\max}|NC,S_a}(s_a^2)$. We have plotted in Figure 5-15 the drift hazard for drift values near drift values, $\hat{\eta}_{\theta_{\max}|NC,S_a}({}^{P_o}s_a)$ and $\hat{\eta}_{\theta_{\max}|NC,S_a}(s_a^2)$. The final step is to find the drift value that corresponds to a hazard value equal to $p_o = 0.0088$. It is estimated to be 0.018 (Figure 5-15, heavy line). If we use the non-parametric method to calculate the factored demand corresponding to an allowable probability of $p_o = 0.0088$, we get a value equal to 0.025 (Figure 5-15, light line). We can enhance the former estimate by selecting a new s_a level higher than 0.7g. However, in this case study, the median conditioned on no collapse displays abrupt changes at spectral accelerations larger than 0.70g

(Figure 5-6). This will cause the resulting drift hazard curves to be less reliable for intensity levels larger than 0.70g.

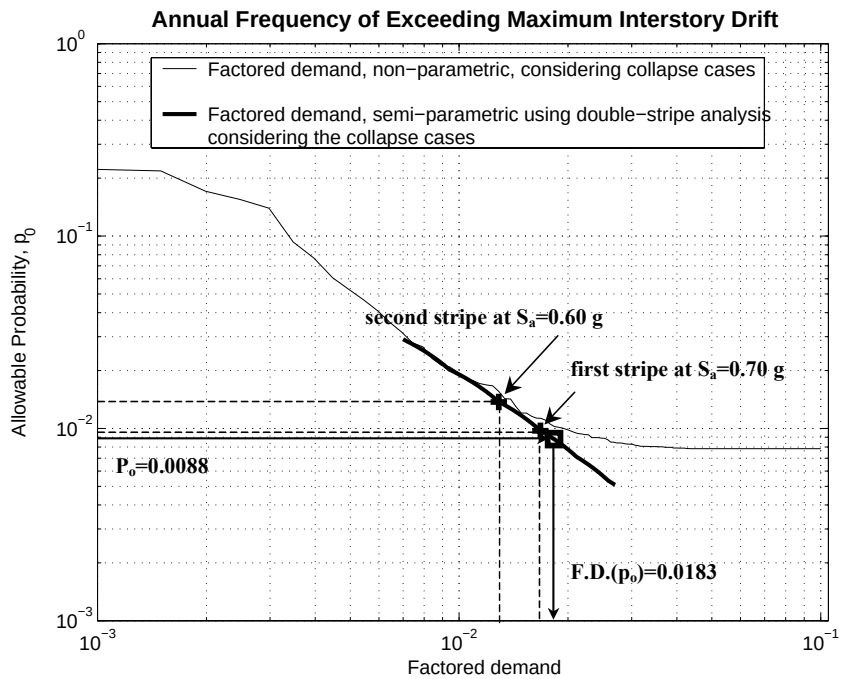

Figure 5-15 - Double-stripe, semi-parametric factored demand estimation: Using the closed-form drift hazard in Equation 5-23 considering the collapse cases, with results for $S_a = 0.6g$ and $S_a = 0.70g$ and non-parametric spectral acceleration hazard.

It can be observed that the drift hazard estimated using double-stripe analysis is fairly close to the non-parametric drift hazard for a range of drift values in the vicinity of the conditional median values for the two stripes given non-collapse, $\hat{\eta}_{\theta_{\max}|NC,S_a}(^{P_o}s_a)$ and $\hat{\eta}_{\theta_{\max}|NC,S_a}(s_a^2)$, e.g., drift values as large as 1.6%. The drift hazard curve starts to diverge from the non-parametric drift hazard curve, as the drift values get closer to the collapse regime. It should be mentioned that this description has presented that collapse could be recognized from single-stripe analysis. This would be true if collapse is defined by non-convergence or an excessive (unreasonable) displacement. If, however, it is defined by the shape of the IDA, then more than one analysis of each record is needed to define the collapse capacity. Clearly these runs can be of value in the over-all drift hazard and/or factored demand analysis. While a systematic method to search efficiently for IDA-based capacities exists (Vamvatsikos and Cornell, 2001), there are no

algorithms as yet that treat global capacity estimation and drift hazard/factored capacity estimation together in a coordinated manner.

5.8.5 Discussion

Several methods for estimating the displacement-based demand (the engineering demand parameter) in the collapse regime were discussed. These methods employ the proposed generalized definition of the factored demand. In this definition, the factored demand for the allowable probability, p_o, is equal to the drift value that has an annual frequency of exceedance (hazard), $\lambda_{\theta_{\max}}$, equal to p_o. Based on this property, any drift hazard curve is also a factored demand curve where the hazard axis is the same as the allowable probability axis and the drift axis is the same as the factored demand axis. The non-parametric method for estimating the factored demand makes use of the above property to estimate the factored demand from the non-parametric drift hazard curve considering the collapse cases. This is the most accurate method for demand estimation studied in this chapter. Other methods considered include the fully-parametric method that uses the pseudo-parametric IDA percentiles to obtain the required parameter estimates in order to calculate the factored demand from the simple DCFD format (see Chapter 4). Comparing the results of the fully parametric method with the non-parametric one, we can observe that the fully-parametric method provides a smooth and accurate approximation to the non-parametric results as long as a fully-parametric estimate for median is available (Figurer 5-13). The relatively small computational effort involved in the fully parametric method together with the simplicity of the DCFD formulation (Equation 5-26), makes this an efficient alternative to use.

The next method studied in this section is the semi-parametric method using the fully parametric IDA curves. This method is very similar to the one studied before apart from the fact that it incorporates the local parameter estimates derived from the parametric IDA curves into the formulation for the drift hazard considering the collapse cases (Equation 5-23). This method better captures the close-to-collapse part of the drift hazard. Finally, a semi-parametric method using a minimal number of stripes is discussed. This method is being presented in the form of a step-by-step procedure for the local estimation of the drift hazard/factored demand. The advantage of this method is that it uses few stripes (typically two) to obtain parameter estimates for the drift hazard curve considering the collapse cases. This method is not very accurate in this example.. The inaccuracy can be attributed to the less-than-smooth behavior of the given no collapse median at intensity levels larger than 0.7g.

5.9 Factored capacity

Similar to factored demand, the factored capacity was defined in Chapter 4 in the context of the demand and capacity factored design as:

$$\text{factored capacity} = \text{median capacity} \times \text{the capacity factor}$$

Alternatively, the factored capacity can be defined as the drift value with a frequency of exceedance equal to the limit state frequency. In other words, the factored capacity is the drift value corresponding to a frequency equal to the limit state frequency from the drift hazard curve. For example, the factored capacity derived from the drift hazard considering the collapse cases (e.g., Figure 5-10) lies at infinity. This is because the frequency of the collapse limit state is the right asymptotic value for the drift hazard considering the collapse cases. The drift hazard considering the collapse cases should however be used for the estimation of factored capacity values that correspond to limit states other than collapse, called here the "exogenous" limit states, e.g., the immediate occupancy limit state or a local member failure limits state short of collapse due to global instability. It should be noted that the same information that is used to derive the drift hazard considering the collapse cases is used to calculate the collapse limit state probability. Thus, the drift hazard considering the collapse cases cannot be used to estimate the factored capacity for the collapse limit state. It should be noted that this definition of factored capacity, although it is theoretically sound, has very little practical use. However, there are many ways to define the factored capacity as long as it is equal to factored demand at $P_0 = P_f$. Therefore, there still is room for introducing more practical propositions for factored capacity.

5.10 Practical Applications

The methods proposed in this chapter can be used for reliability assessments for "exogenous" limit states, (i.e., other than global instability induced collapse). The formulation presented in this chapter already takes into account this collapse information yielding the probability of limit state as an asymptote of the drift hazard curve (Figure 5-10). Reliability assessments for a single limit state can be performed by obtaining local parameter estimates. By local, we mean a region that is close to the onset of the limit state under investigation. In order to ensure that the estimates are obtained close to the onset of the limit state under consideration, a re-iteration of the analyses might become necessary especially if the structure is in the global collapse sensitive regime. It is shown that in this regime these local estimates can be provided by means of performing a double-

stripe analysis. A procedure for both locating and performing the double-stripe analyses is discussed. It was demonstrated in the previous chapter that the single-stripe analysis could be used for reliability assessments for a single limit state, provided that a reasonable value for the slope parameter b could be assumed. However, acquiring a (local) estimation of parameter b required at least a second stripe. If the collapsing cases are considered in the modeling, there will be more parameters to estimate compared to the simple DCFD formulation derived in Chapter 3. Also, unlike in the previous chapter, the formulation of drift hazard considering the collapse information is not invertible with respect to the drift values. These factors add to the difficulty of reliability assessment based on the results of a single stripe analysis. Performing a double-stripe analysis can be expected to enable us to estimate all the necessary parameters in order to estimate the drift hazard or factored demand in the region of global instability.

Reliability assessment for multiple limit states requires the use of wide-range methods such as the MSA or the IDA procedure (as presented in Chapter 4). In the case of IDA procedure, it is demonstrated here that the analysis effort can be reduced by approximating the individual IDA curves by parametric functions. Parametric approximations of IDA curves are obtained by implementing the results of linear regressions performed on the individual IDA curves into the three-parameter formulation. The number of points required for each IDA curve in order to get these parametric estimates can be as low as 4 points. The first two points are needed in order to estimate the non-collapse intercept and slope of the IDA curve in the logarithmic space. A minimum of two additional points in needed in order to find the global stability limit state capacity point according to a procedure proposed by Vamvatsikos and Cornell, 2002, for locating the capacity points. This procedure uses spline fits to the IDA curves in order to predict the limit state capacity point (see Vamvatsikos, 2002).

5.11 Summary and Conclusions

The conditional probability distribution of drift given spectral acceleration is developed by using the total probability theorem in the range of drift values close to collapse (Equation 5-6). Collapse is defined as the onset of global dynamic instability in the structure marked by the point where the slope of the IDA curve (see Chapter 4, or Vamvatsikos and Cornell, 2001) is reduced to a certain percentage of its initial slope. A proposed parametric representation of this conditional probability distribution is called the three-parameter distribution (see Shome and Cornell, 1999) in order to account for the fact that the probability distribution of drift given spectral acceleration

prior to the occurrence of collapse can be modeled by a lognormal (two-parameter) distribution and the fraction of the collapse cases observed in the data-set can be defined by a third parameter.

Nonlinear dynamic procedures are used with the derived formulation in order to estimate the distribution of the drift given spectral acceleration in the collapse range. The alternative methods for the estimation of the probabilistic distribution of drift response given spectral acceleration can be differentiated based on whether they are derived fully-parametrically, semi-parametrically or non-parametrically. As a special application of the three-parameter distribution, parametric IDA curves and the parametric IDA percentiles are derived for the drift values close to collapse. Alternatively, the results of multiple-stripe analysis (see Chapter 4) are post-processed in order to be implemented in the three-parameter distribution. The resulting semi-parametric percentiles show good agreement with the counted percentiles that were derived in the previous chapter without special consideration of collapse cases. The distribution of drift demand for a given spectral acceleration can also be estimated empirically (non-parametrically) based on the results of multiple-stripe analysis. The advantage of estimating the distribution non-parametrically is that it avoids prior assumptions about the shape of the distribution.

The alternative drift demand estimation methods discussed above are then used in order to derive the annual frequency of exceeding a certain drift value. The result is known as the drift hazard. The non-parametric probability distribution for the drift demand is used to calculate the drift hazard by numerical integration. The result is used as a standard by which the estimates provided by other approaches are compared. Similar to the demand estimation procedures studied in this chapter based on the three-parameter distribution, the alternative methods for the estimation of the drift hazard can be differentiated based on whether they are derived fully parametrically, semi-parametrically or non-parametrically. Parallel to the closed-form solution for the drift hazard in the previous chapter, a fully parametric closed-form for the drift hazard is derived. In practice it is desirable to avoid the close multiple stripes used in this research effort as they require intensive computational effort. As shown in Chapter 4, the single-stripe analysis can be used to estimate the drift hazard from the derived closed-form for a specific drift value, provided that the displacement-based response is not in the region of global instability. It is demonstrated here that utilizing the carefully designed double-stripe analysis in the closed-form solution for drift hazard can provide fairly good local estimates of the drift hazard, in the large drift regime when a large fraction of the records here cause collapse.

The factored demand for a given allowable probability, p_o, can be defined as the drift value with p_o probability of exceedance (see Chapter 3). This definition is used to estimate the factored demand from the estimated drift hazard curve(s). Therefore, factored demand can be estimated non-parametrically from the non-parametric drift hazard curve derived by numerical integration.

The parametric IDA percentiles for drift values close to collapse can be used to estimate the factored demand from the simple (two-parameter) closed-form formulation for DCFD format derived in Chapter 3 (Equation 5-26). Factored demand calculated for multiple allowable probability levels, p_o, is compared to the non-parametric factored demand. The results show very good agreement as long as the parametric IDA percentiles are still available. Alternatively, the parametric IDA curves can be incorporated in the closed-form drift hazard derived based on the three-parameter distribution (Equation 5-23). The resulting factored demand calculated for multiple allowable probability levels have been compared to the corresponding non-parametric estimates for factored demand and the results indicate good agreement. This agreement between the parametric factored demand derived from the closed-form drift hazard curve and the non-parametric results is particularly desirable since the parametric factored demand can be obtained with considerably less analysis effort than the non-parametric factored demand. In an attempt to estimate the drift hazard locally, a double-stripe method (see Chapter 4) was used. The double-stripe method was used in order to provide parameter estimates for the drift hazard in Equation 5-23. The resulting estimate for drift hazard by following this approach was fairly close to the non-parametric results. Nonetheless, this method needs to be tested for a variety of ductility ranges in order to test its robustness.

5.12 Acknowledgements

The authors would like to acknowledge the Pacific Earthquake Engineering Research Center, PEER, funded by the U.S. National Science Foundation.